Modeling of Retinal Ganglion Cell Responses to Electrical Stimulation with Multiple Electrodes

L.A. Hruby
Salk Institute for Biological Studies

Introduction

Since work on epiretinal electrical stimulation for vision restoration began in the 1980s, it has become clear that development of an implantable epiretinal prosthesis that can restore vision to a level at which significant visual tasks, such as face recognition and reading, is feasible. The transmission of meaningful visual information from the prosthesis to the central nervous system is central to the success of such prostheses. This transmission can be achieved by controlling the firing of retinal ganglion cells (RGCs) using electrical fields created by current injected on the inner surface of the retina. In order to induce the same activity that occurs during normal vision, this control must have single-cell specificity.

Individual RGCs have been stimulated using single micron-scale electrodes in isolated mammalian retina.[1] However, it is unlikely that stimulation with single electrodes will be capable of specifically stimulating each RGC in the retina due to the high density of RGCs, particularly in the central regions of the retina. In order to selectively stimulate cells with an electrode array that has a lower electrode density than the density of the targeted cells, specific combinations of electrodes must be chosen that maximize selectivity of the targeted cells. However, the effect of stimulation with combinations of electrodes on the response of RGCs is unknown. Experimental evidence (not shown) suggests that the response of a retinal ganglion cell to current injection through a pair of electrodes may not be predictable based only the responses of the cell to stimulation by each of the electrodes individually.

The purpose of this study was to model the effects of using combinations of micron-scale disc electrodes to stimulate an individual RGC. In particular, the study will examine the relationship between the sensitivity of an RGC to current injection through individual electrodes and through pairs of electrodes.

Materials and Methods

The standard cable model, with constant membrane conductances, was used to simulate the effect of extracellular potential distributions on membrane potential **(Figure 1)**. Since there were no voltage-dependent conductances in the model, the resting potential of the membrane was reduced to zero and all membrane potentials were calculated with respect to this reduced membrane potential. In this model, the change in membrane potential at node *i* is defined by applying Kirchoff's current law at each node **(equation 1)**, with V_m denoting membrane potential, G_m and G_a denoting membrane and cytoplasmic conductances, respectively, C_m denoting membrane capacitance, and V_{ext} denoting the external potential. At segment ends and intersections of three or more segments, terms were dropped and added to account for the different number of current sources.

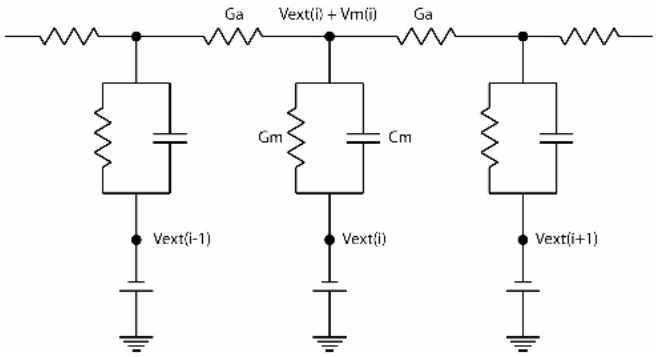

Figure 1: **Standard cable model**. A capacitance C_m and constant conductance G_m in parallel represent the membrane of the cell at each node, separating the external potential $V_{ext}(i)$ from the internal potential, which is the sum of the external potential and the transmembrane potential $V_m(i)$. External potential at each node is determined by equations **(2)** and **(3)**, using the coordinates of the center of the neural element represented by the specified node. Neighboring intracellular nodes are connected by a cytoplasmic conductance G_a.

(1) $$\frac{dV_m(i)}{dt} = \frac{1}{C_m}\left[-G_m V_m(i) + G_a\left(V_m(i+1) - 2V_m(i) + V_m(i-1) + V_{ext}(i+1) - 2V_{ext}(i) + V_{ext}(i-1)\right)\right]$$

Values for membrane and cytoplasmic conductances of each element were based on the measured membrane (50,000 Ωcm^2) and cytoplasmic resistivities (110 Ωcm) of amphibian retinal cells.[2] A membrane capacitance of 1 μF/cm^2 was used to calculate capacitance for each model element.

The morphology of the modeled retinal ganglion cell was based on a sketch of a human outer midget retinal ganglion cell from mid-peripheral retina described in Dacey 1993 **(Figure 2A)**.[3] The cell was given a third dimension by choosing random y-coordinates coordinate for each segment intersection or end, and then refining the random values until the cell appeared realistic, based on the assumption that the dendritic spread was roughly radially symmetric. The cell was broken into 44 individual segments: an axon, an initial segment, five somal segments, and 37 dendritic segments. Each segment was assigned a length and constant diameter based on the sketch, and discretized into ten individual cable elements, each characterized by an external potential and a transmembrane potential. Only five dendritic segments were used in the simulations due to instability of the simulation.

Extracellular potentials for each cable element were calculated using an analytical solution to Laplace's equation for current flow from a conductive disc electrode into a homogeneous, purely resistive, semi-infinite slab, with a ground electrode at infinity. [4]

(2) $$V_o = \frac{I_0}{4\sigma a}$$

(3) $$V(r,z) = \frac{2V_0}{\pi}\sin^{-1}\left\{\frac{2a}{\left[(r-a)^2 + z^2\right]^{1/2} + \left[(r+a)^2 + z^2\right]^{1/2}}\right\} \quad \text{for} \quad z \neq 0$$

Here, I_o is the injected current amplitude, V_o is the quasi-static potential on the electrode surface, σ is the conductivity of the tissue, a is the radius of the electrode (2.5 μm in all simulations), and the cylindrical coordinates r and z are with respect to the center of the electrode. The conductivity of cat cortex, 1/222 S/cm,[5] was chosen for this study based on the structural similarities between retinal tissue and cerebral cortex.

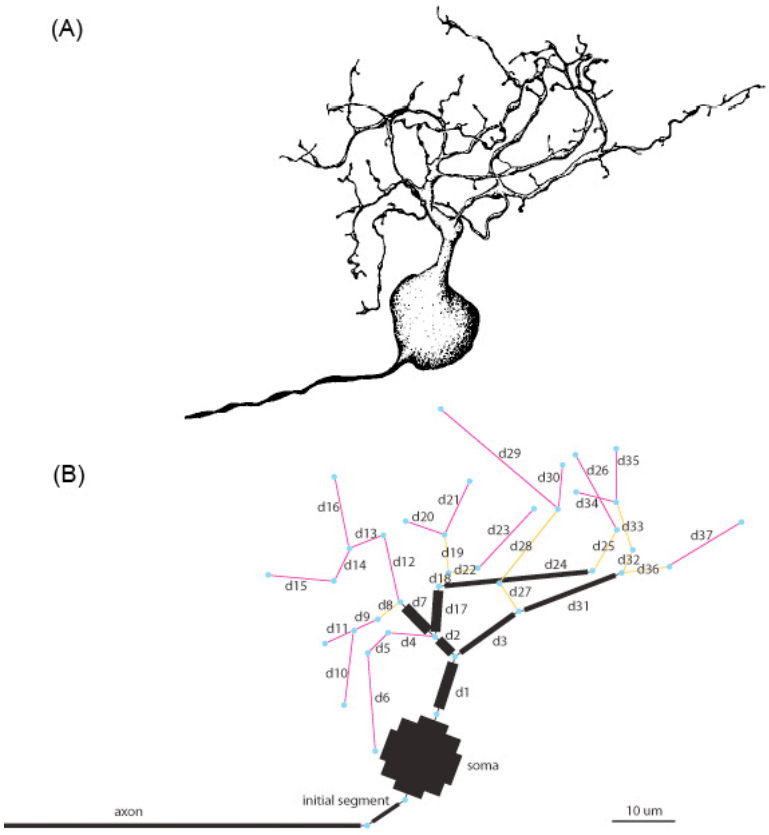

Figure 2: Human midget ganglion cell and model morphology. (A) Sketch of a human midget ganglion cell from Dacey 1993. (B) Model of retinal ganglion cell based on sketch. Each labeled segment is modeled as a cable with ten nodes. The soma has four additional nodes with distinct diameters. Black segments have individual diameters based on measurements of the sketch. Pink segments have 0.8 um diameters, and yellow segments have 0.9 um diameters.

Membrane potentials at each time point were determined using a finite difference method. Current flow to and from each intracellular potential node at each time point was calculated and used to update the transmembrane voltage values for the next time point. The length of time step used was 500 picoseconds.

Results

The membrane potentials resulting from a 100 μs application of external potential distributions calculated from equations (2) and (3) based on current injection of -5μA through individual electrodes and pairs of electrodes for two electrode configurations is shown in figure 3. Based on the idea that depolarization of a portion of the active membrane of a neuron triggers action potential generation if depolarization surpasses a threshold potential region, the peak depolarization levels of the membrane in regions where action potentials initiation is possible (soma, initial segment, and axon) were used to infer the relative sensitivity of the cell to stimulation with each of the simulated electrode configurations.

Electrodes placed directly below the soma or near the axon (configuration A, figure 3A) had the greatest peak depolarizing effect on the modeled cell. Peak depolarization values for simulated stimulation with electrodes in configuration A were 34.6 and 47.0 mV, respectively. The peak depolarization for stimulation with both electrodes 1 and 2 simultaneously was 40.7 mV, 18% higher than for electrode 1 alone but 13% lower than for electrode 2 alone.

Simulated stimulation with electrodes placed in configuration B (figure 3B) had a much smaller depolarizing effect on the cell, with peak values of 13.5 and 11.9 mV for electrode 1 alone and electrode 2 alone, respectively. Simulated current injection through both electrodes simultaneously resulted in a large increase in peak depolarization in this configuration, resulting in 25.4 mV depolarization in one node of the initial segment. This was an increase of 88% from stimulation with electrode 1 alone and 113% from stimulation with electrode 2 alone.

Discussion

As is clear from this study as well as several other electrical stimulation modeling studies,[6-8] the effect of extracellular current injection is likely to have a complex effect on the cells membrane potential, depolarizing the membrane in some regions will hyperpolarizing the membrane in other regions. As a linear system, the membrane polarization distribution resulting from current injection through combinations of electrodes is simply the sum of the membrane polarization distributions resulting from current injection through each of the electrodes individually. However, the probability of evoking an action potential is likely to be more closely tied to the maximum depolarization of the active region of the membrane than the entire polarization distribution. This study has shown that the maximum depolarization achieved by injecting current through combinations of electrodes is not expected to be a linear sum of the maximum depolarization achieved using individual electrodes.

The results of this study suggest that the distribution of membrane polarization is crucial in determining how the peak depolarization value induced by current injection through a combination of electrodes depends on the peak depolarization induced by current injection through the constitutive electrodes. Distributions that are similar, such as those induced by

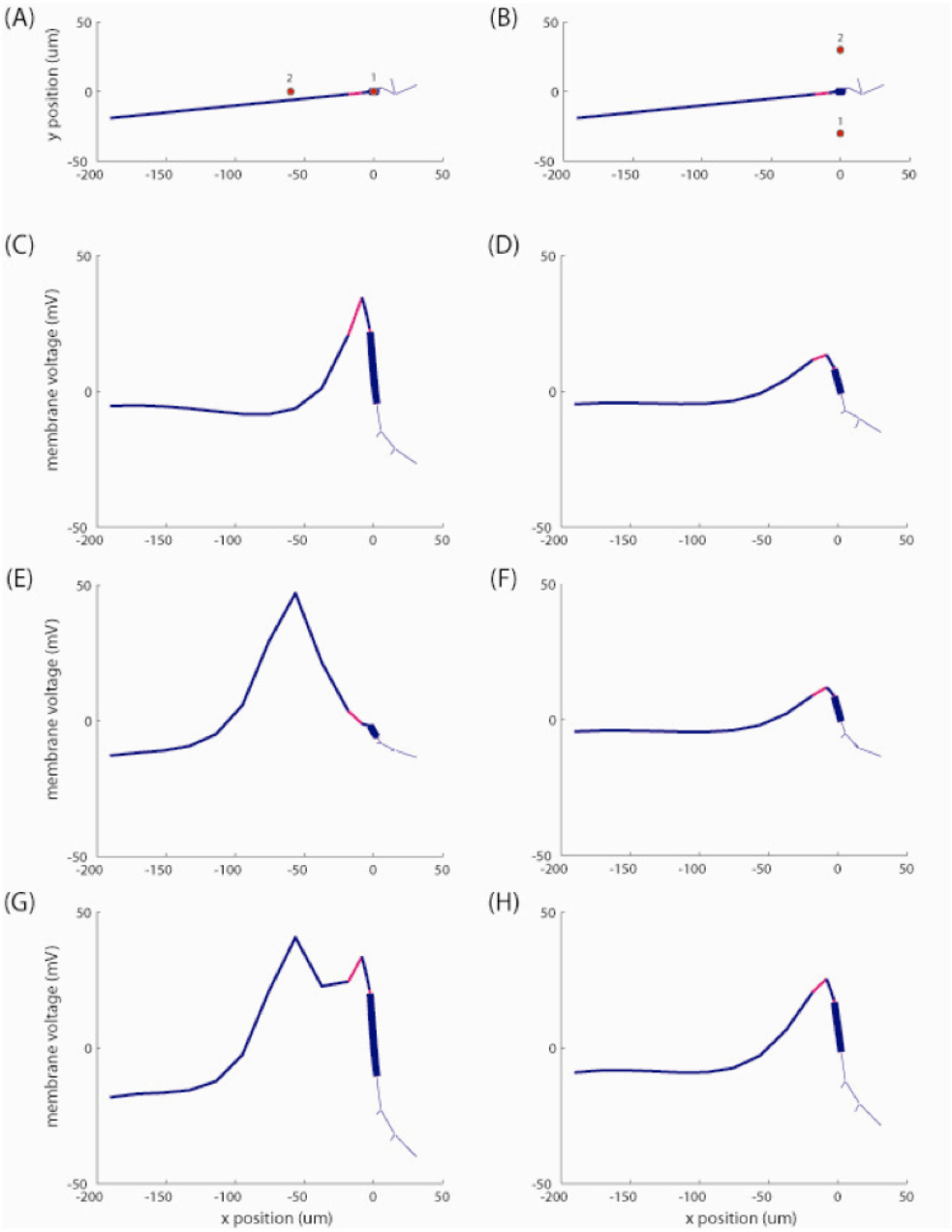

Figure 3: Effects of stimulation with combinations of electrodes on membrane potential. (A) (B) Top view of positions of electrodes relative to RGC in configurations A and B. All electrodes lie in a plane 30 μm below the center of the soma. (C)-(H) Membrane potential as a function of position at the end of a 100 μs, -5 μA simulated current pulse injected through individual or multiple electrodes. Results for current injection through (C) electrode 1 of configuration A., (D) electrode 1 of configuration B, (E) electrode 2 of configuration A, (F) electrode 2 of configuration B, (G) electrodes 1 and 2 of configuration A, and (H) electrodes 1 and 2 of configuration B.

current injection through electrodes 1 and 2 of electrode configuration B, "constructively interfere" with each other, leading to near-linear summation of peak depolarization. Conversely, dissimilar distributions may lead to little increase in peak depolarization when summed, or may even "destructively interfere" with each other in cases were hyperpolarized regions induced by stimulation with one electrode overlap depolarized regions induced by stimulation with another electrode. This was the case when current was injected through electrode 1 in addition to electrode 2 of configuration A. The region of peak depolarization in induced by stimulation with electrode 2 overlaps a region of hyperpolarization induced by stimulation with electrode 1, causing a decrease in peak depolarization when current is injected through both electrodes simultaneously.

Determining optimal electrode combinations for achieving single-cell specificity of electrical activation of RGCs requires knowledge of how the effects of current injection through individual electrodes combine to induce a specific response. The potential for spike generation in multiple regions of a neuron makes it difficult, if not impossible, to predict the responses of a neuron to stimulation using a combination of electrodes based on the responses of the neuron to the constitutive electrodes alone. In order to predict whether stimulation by one electrode will constructively or destructively interfere with stimulation by another, it is necessary to determine which regions of the membrane are being depolarized and hyperpolarized. Future studies will focus on methods for predicting the location of electrically-induced action potential initiation, based on other characteristics of a cell's responses to electrical stimulation, such as response latency.

References

1. Sekirnjak, C. *et al*. Electrical stimulation of mammalian retinal ganglion cells with multielectrode arrays. *J. Neurophysiol.* **95**, 3311-3327 (2006).

2. Coleman, P A Miller,R F. Measurement of passive membrane parameters with whole-cell recording from neurons in the intact amphibian retina. *Journal of neurophysiology* **61**, 218 (1989).

3. Dacey, D. M. The mosaic of midget ganglion cells in the human retina. *The journal of neuroscience* **13**, 5334 (1993).

4. Wiley, J D Webster,J G. Analysis and control of the current distribution under circular dispersive electrodes. *IEEE transactions on bio-medical engineering* **29**, 381 (1982).

5. Geddes, L A Baker,L E. The specific resistance of biological material--a compendium of data for the biomedical engineer and physiologist. *Medical biological engineering* **5**, 271 (1967).

6. Schiefer, Matthew A Grill,Warren M. Sites of neuronal excitation by epiretinal electrical stimulation. *IEEE transactions on neural systems and rehabilitation engineering* **14**, 5 (2006).

7. Rattay, F. The basic mechanism for the electrical stimulation of the nervous system. *Neuroscience* **89**, 335 (1999).

8. Rattay, F. R., Susanne. Effective electrode configuration for selective stimulation with inner eye prostheses. *IEEE transactions on bio-medical engineering* **51**, 1659 (2004).